Geomorphology 248 (2015) 111–124

Contents lists available at ScienceDirect

Geomorphology

journal homepage: www.elsevier.com/locate/geomorph

Morphological perspective on the sedimentary characteristics of a coarse, braided reach: Tagliamento River (NE Italy)

Emanuel Huber *, Peter Huggenberger

Applied and Environmental Geology, University of Basel, Bernoullistrasse 32, 4056 Basel, Switzerland

ARTICLE INFO

Article history:
Received 21 October 2014
Received in revised form 6 July 2015
Accepted 7 July 2015
Available online 20 July 2015

Keywords:
Braided river
Morphology
Preservation potential
Heterogeneity
Subsurface flow
Tagliamento River

ABSTRACT

In order to understand heterogeneity distribution of hydraulic properties, many studies have proposed models of coarse, braided river deposits. However, they often focus either on the surface/near surface or on ancient deposit analysis. Furthermore, the link between morphological (surface) and sedimentological (outcrops) information has not been fully explored yet. This publication aims to characterize the morphodynamics of a braided, gravel-bed reach of the Tagliamento River (NE Italy) and to assess its relationship with the subsurface heterogeneity. The morphological analysis is based on a LiDAR-derived DEM, aerial and satellite photographs from 1998 to 2011, as well as field observations. A water-stage time series allows the morphological changes to be related to the discharge dynamics. The sedimentological knowledge on coarse, braided deposits was mainly gained from the observation of analog Pleistocene coarse deposits in Switzerland. The main geomorphological elements are identified in terms of their topographic signature and genesis, setting apart the trichotomy water–vegetation–bar. The braidplain is characterized by higher-lying zones with dentritic gully drainage networks and active zones where most of the morphology reworking occurs. Furthermore, two morphologies mark the active zones: a low-discharge morphology (low-discharge incisions and channels, slip-face lobes, etc.) superimposed on a high-discharge morphology (gravel sheets, scours, etc.). Each morphological element is related to a depositional (i.e., sedimentological) element whose preservation potential in the subsurface is assessed as a function of the river-bed aggradation dynamic. The settings that impact the subsurface flow in terms of fast pathway and connectivity are addressed.

1. Introduction

The highly dynamic depositional and erosional processes of coarse, braided rivers (Ashmore and Parker, 1983) have formed heterogeneous deposits that make up many of the European and North American groundwater reservoirs (Huggenberger and Aigner, 1999; Klingbeil et al., 1999; Bayer et al., 2011). These deposits often show large variation in hydraulic conductivity and porosity (e.g., Jussel et al., 1994; Webb and Anderson, 1996; Anderson et al., 1999; Klingbeil et al., 1999; Heinz et al., 2003). Therefore, characterizing the heterogeneity of coarse, braided river deposits is an important prerequisite to reliable subsurface flow and transport simulations (Bayer et al., 2011).

A broad knowledge is available on the sedimentology of alluvial deposits and its related concepts (e.g., Allen, 1978; Miall, 1985; Best and Roy, 1991; Heller and Paola, 1992; Paola et al., 1992; Brierley and Fryirs, 2005). For example, Ashmore and Parker (1983) showed with laboratory experiments and field observations the importance of factors such as braiding intensity and scouring on sedimentation in braided systems. Anderson (1989), Anderson et al. (1999), and Klingbeil et al. (1999) related the concept of lithofacies to hydrofacies in fluvial environments for studies on groundwater flow and transport. The addition of shallow geophysical methods such as high-resolution ground penetrating radar (GPR) has been very effective in outlining the relevant hydrofacies (Best et al., 2003). Lunt et al. (2004) and Bridge and Lunt (2006) combined GPR data with data from trenches, cores, logs, and permeability/porosity measurements in a study of a three-dimensional depositional model of a braided river system.

Although lithofacies descriptions of braided river deposits are becoming more and more detailed (Bayer et al., 2011), conceptual models of coarse, braided river deposits focus either on the low-discharge streams and on the surface/near surface (e.g., Webb, 1994; Bridge and Lunt, 2006; Ramanathan et al., 2010; Colombera et al., 2013; Pirot et al., 2014) or concentrate on sedimentological descriptions based on vertical outcrop analysis (e.g., Sun et al., 2008; Comunian et al., 2011).

Despite the efforts to understand braided river systems and the resulting subsurface heterogeneity patterns, some fundamental aspects of the dynamics of these systems are not fully explored yet, in particular the link between morphological (surface) and sedimentological (outcrop) information (Sambrook Smith et al., 2006). The dynamics of

* Corresponding author.
E-mail addresses: emanuel.huber@unibas.ch (E. Huber), peter.huggenberger@unibas.ch (P. Huggenberger).

http://dx.doi.org/10.1016/j.geomorph.2015.07.015
0169-555X/

braided rivers is a key to understanding the preservation potential of characteristic depositional elements and the resulting subsurface sedimentary textures and structures (Huggenberger and Regli, 2006). The relationship between the river-bed morphology and the turbulent flow leads to sorting processes that form sediment units with a characteristic permeability (Best, 1993). The spatial distribution and the geometry of the preserved depositional elements themselves control the connectivity of high/low permeable units and, therefore, can strongly influence the hydraulic heterogeneity patterns (e.g., Anderson et al., 1999; Lunt et al., 2004; Comunian et al., 2011). The challenge in this context is to find a relationship between the present morphology of braided river systems and the geometry of architectural elements of ancient deposits (e.g., Siegenthaler and Huggenberger, 1993; Bristow and Jol, 2003; Kelly, 2006).

The present work aims to characterize the morphodynamics of a gravel-bed braided reach of the Tagliamento River (northeast Italy) and to assess its relationship with sedimentary records. We seek to better understand the subsurface hydraulic heterogeneity as a function of the morphodynamics for subsurface flow and transport simulations.

Many large European rivers are strongly regulated and the geomorphological and sedimentological processes that built up their floodplains are no longer observable. In contrast, the Tagliamento River is almost morphologically intact and constitutes a model reference for highly dynamic natural rivers (Ward et al., 1999). Therefore, the Tagliamento River represents an ideal field laboratory to study the relationship between surface morphology and subsurface heterogeneity.

Specifically, we attempt (i) to identify the main geomorphological elements in terms of their topographic signature and genesis (we set aside the planform trichotomy *water–vegetation–bar*); (ii) to quantify the geomorphological effectiveness of the flood events and therefore the rate of turnover of the main geomorphological elements; (iii) to relate the morphological elements with depositional elements, i.e., to assess how the morphological elements are reworked/filled and buried in the sedimentary records; and (iv) to assess the preservation potential of the main depositional elements in the subsurface as a function of the river-bed aggradation dynamic.

The analysis is based on a LiDAR-derived DEM, aerial and satellite photographs as well as on-field observations of the Tagliamento River and of gravel pit exposures of Pleistocene coarse deposits in Switzerland.

2. Study site

The Tagliamento River is one of the last large seminatural rivers of the Alps (Ward et al., 1999). The 170-km-long Tagliamento River is located in the Friuli Venezia Giulia region, northeastern Italy. Its source lies in the Carnian Alps at the Mauria Pass (1195 m asl) and flows into the Adriatic Sea. The 2500-km^2 catchment of the Tagliamento is funnel-shaped. The headwaters are characterized by an alpine climate, whereas the lower reach is characterized by a Mediterranean climate. Consequently, the discharge regime of the Tagliamento is highly variable (Bertoldi et al., 2009). From its source to Varmo (Venetian–Friulian plain), the Tagliamento River is mostly gravelly braided and is locally confined by bedrock gorges and narrows, often because of thrust tectonics. Slope differences between different river reaches can lead to either aggrading or degrading river reaches. Therefore, marked differences in preservation potential of the main depositional elements are to be expected over relatively short distances.

For our study, we are primarily interested in the partly confined valleys in the external part of mountain ranges and foothills, as the dynamics are comparable to important large valleys in similar structural settings: they are akin in terms of gravel and sand proportion, and lateral sediment migration dominates over longitudinal transport.

The present work focuses on the 6.5-km-long Cimano–Pinzano reach delimited at the upstream end by the Cimano bridge and downstream by the Pinzano gorge (Fig. 1). The Cimano bridge is built on a large, stable wooded island with a center formed by a 100-m-narrow and 600-m-long Tertiary conglomerate (Cucchi et al., 2010). The Tagliamento flows around both sides of the bedrock island. The 125-m-wide Pinzano gorge is located at the southernmost foreland thrust in the subalpine molasses and confines the Tagliamento River into a more or less single-thread stream before it flows into the Venetian–Friulian plain. At the Pinzano gorge, the catchment area of Tagliamento River reaches 85% of the whole catchment area. The southeastern side of the braidplain is confined by Tertiary conglomerates of the foothills of Mount Ragogna. The western flank bounds an inactive fluvial terrace (100 to 900 m wide) lying 20 m above the present active alluvial plain. The Tagliamento River has a braided pattern at low discharge between the Cimano bridge and the Pinzano gorge. The braidplain (3.8 km^2) is up to 1 km wide and is characterized by the presence of a few large wooded islands. Thus, this reach was classified as island-braided by Ward et al. (1999). The Arzino tributary (catchment size of 120 km^2) enters the Tagliamento River at Flagogna.

As a result of the active thrusting of southern subalpine molasse onto the Venetian–Friulian plain (active foreland thrust system; Bechtold et al., 2009), the elevation of the bedrock surface at the Pinzano gorge acts as a base level, influencing the aggradation/degradation history of the Cimano–Pinzano reach. Recent neotectonic structures near the Pinzano gorge would favor an aggradation of the Cimano–Pinzano reach in the timescale of hundreds to several thousands of years (timescale of landscape-shaping tectonic events in the area; see Burrato et al., 2008; Bechtold et al., 2009). However, the analysis of aerial photographs indicates a more complex aggradation–degradation dynamic within the river reach at the decadal timescale caused by variable flood frequency, sediment supply including anthropogenic influences of gravel exploitation, and vegetation changes in the surrounding areas and upstream.

Previous studies based on historical aerial photographs and field observations showed that the morphological evolution of the Cimano–Pinzano reach is highly dynamic. Zanoni et al. (2008) analyzed historical aerial photographs of the Cimano–Pinzano reach (among others) over a period of 60 years. They concluded that established islands are 'remarkably transient features' as they did not survive for more than 23 years. Van Der Nat et al. (2003) mapped the different types of habitats over 2.5 years and concluded that 'more than 59% of the aquatic area and 29% of vegetated islands were restructured'. Bertoldi et al. (2009) related the river stage frequency to inundation and morphological shaping. Their wavelet analysis of the water stage series recorded at the Villuzza gauging station (downstream from the Pinzano gorge) between 1981 and 2006 showed that the water stage fluctuations were very irregular and not significantly influenced by anthropogenic interventions. Furthermore, they deduced that flow stages above 300 cm (at the Villuzza gauging station) were 'required to significantly erode floodplain and island margins or to cut avulsion channels that dissect new islands from the floodplain' (Bertoldi et al., 2009). Welber et al. (2012) analyzed the response of morphological features of the lower part of the reach to flood events. Using automated high-frequency photographic records over two years (2008–2009), they observed that the low-discharge patterns were confined to 46% of the studied subreach and that short-lived water bodies represented 30% of the wetted area. Small changes in the vegetation distribution were documented as well as 'a strong link between vegetation distribution and [stream] persistence' (Welber et al., 2012). Recently, Surian et al. (2015) concluded that the turnover between 1954 and 2011 was 'remarkably rapid with 50% of in-channel vegetation persisting for less than 5–6 years and only 10% of vegetation persisting for more than 18–19 years'. They also noticed that low magnitude and relatively frequent flood events (recurrence interval of 2.5 years) significantly eroded the vegetation. Thirteen kilometers downstream from the studied reach Mao and Surian (2010) observed that the lower morphological units and the 'low bars' experienced full gravel removal for high-frequency, low-magnitude floods (i.e., recurrence interval <1 year and 1.1 year, respectively). On the 'higher bars', only partial gravel removal and fine sediment deposition were observed for a flood event with a recurrence interval of 3.5 years.

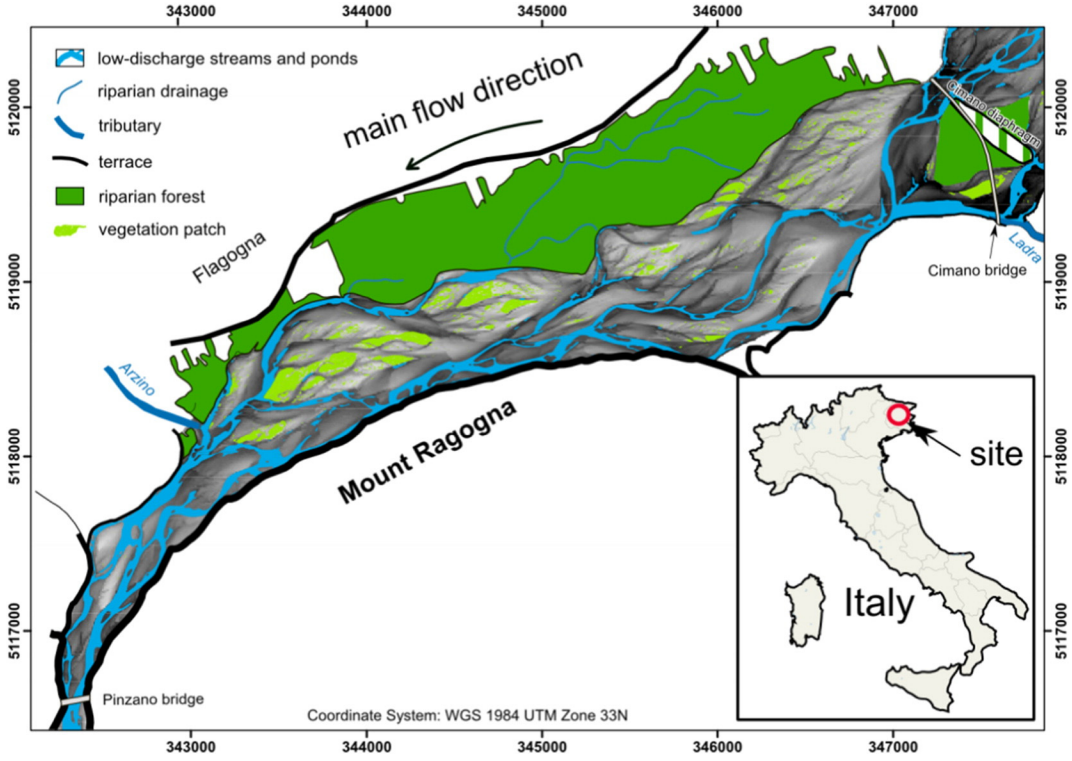

Fig. 1. Overview of the Cimano–Pinzano reach in May 2005. The background of the braidplain is the relative LiDAR-derived DEM.

While most studies on the Cimano–Pinzano reach have focused on morphological and biological processes, the relationship between the morphology and the sedimentary deposits has not drawn much attention.

3. Method

3.1. Data

A water stage time-series for the period 1997–2012 (Villuzza station, downstream from the Pinzano gorge, Servizio Idraulica of the Autonomous Region of Friuli Venezia Giulia, Supplementary Fig. 1 online) allowed morphological changes to be related with the discharge history. The planimetry as well as the morphological analysis of the reach are mainly based on a Quickbird panchromatic photograph from May 2005 (0.5-m resolution, water stage = 50 ± 13 cm), a LiDAR-derived DEM from 23 May 2005 (2.2-m resolution, water stage = 44 cm, surveyed by the U.K. Natural Environment Research Council (NERC) and processed by Bertoldi et al. (2011), and regular field observations since 2009. Orthophotos available online[1] from 1998, 2003, 2007, and 2011 completed our observations. Note that in the LiDAR-derived DEM, the elevation of the wetted parts of the river bed is the water surface elevation and not the elevation of the submerged river bed. The photograph and the DEM look different because the sharp color contrasts on the photograph (e.g., between the water and the sediments) are not necessarily related to sharp elevation changes on the DEM (and vice versa).

3.2. Terminology

The *braided river plain* (or braidplain) is defined as the area that has been subjected to recent morphological changes by the river (see Fig. 2). Bankfull stage refers to the water elevation necessary to completely inundate the braidplain (up to some emergent vegetation patches). The braidplain consists of higher-lying zones (presumably called 'bar assemblages' in Lunt et al. (2004) or 'high bars' in Mao and Surian (2010) and abbreviated to *high zones* hereafter) with a dendritic drainage network surrounded by lower-lying zones called 'lower-lying actively-braiding belt' by Hicks et al. (2002) and abbreviated to *active zone* hereafter, following Gurnell et al. (2000) and Petts et al. (2000).

The connected inundated areas constitute the *low-discharge stream* network, whereas the isolated water bodies are called *ponds*. Note that throughout this paper the term *stream*, without any specification, is used specifically for the *connected inundated areas at the observation time* (i.e., a planform definition that is water-stage dependent). The term *channel* is exclusively reserved to describe rather elongated depressions that have been shaped by flowing water (physical/geometrical definition that is water-stage independent).

The term bar is avoided for the following reasons. (i) Bar is a very general term that describes any type of gravel accumulations that form topographic highs (e.g., American Society of Civil Engineers (ASCE) Task Force, 1966; Smith, 1974). The classification of bars according to their planview shape is not directly related to their sedimentary properties. (ii) In the literature bar refers alternatively to morphologies identified by their topography and/or their planform shape defined by the water shoreline (i.e., shape of exposed gravel areas). Therefore, we use the phrase *gravel sheet* (Todd, 1989; Hicks et al., 2002, 2007; Benn and Evans, 2010) to describe relatively unaltered depositional units of gravel that form sheet-like layers that are elongated in the direction of their formative discharge, rather lobate in planform, and deposited on a former topography (see Figs. 6C, E and 8C). The gravel sheets commonly have an avalanche face at the front and lateral edges; they are a few centimeters to 2 m thick and up to 200 m wide (Hicks et al., 2002). This definition is water-stage independent and refers to a specific depositional process that forms clearly-bounded landforms.

Scours are defined as 'distinct depressions in the river bed caused by erosion processes that are intrinsic to the fluvial channel and result from

[1] WebGIS-application of the Autonomous Region of Friuli Venezia Giulia, URL: http://irdat.regione.fvg.it/WebGIS (last accessed on 6 July 2015), coordinates 344156, 5118590 (ETRS89-TM33).

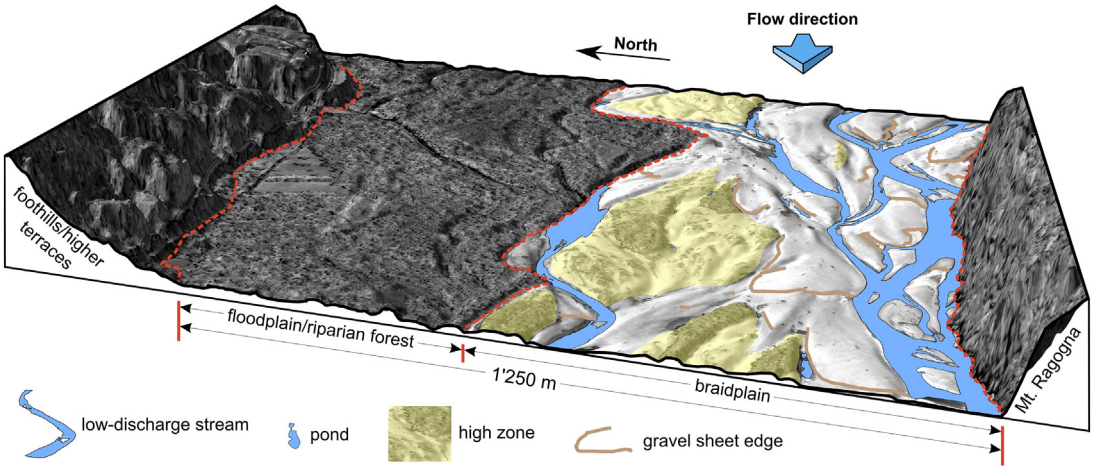

Fig. 2. Portion of the Quickbird photograph projected on the LiDAR-derived DEM. The main morphological elements described in the terminology section are here represented.

changes in hydraulic conditions' (Eilertsen and Hansen, 2007). Scours can be classified into bend, confluence, obstacle, and confinement scours.

3.3. Geomorphology

The LiDAR-derived DEM was detrended to better visualize the braidplain topography and to compare the relative elevations of the morphological features. The longitudinal gradient was estimated by the mean elevation of the braidplain over a disk of a radius larger than the maximal braidplain width and removed from the LiDAR-derived DEM. We used both the relative DEM and the Quickbird photograph combined with our field experiences on the Tagliamento braidplain to map the morphological features observed at low discharge: high and active zones, low-discharge streams, ponds, gravel sheet edges, depositional lobes, etc. We also delineated gravel sheet edges on the orthophoto from 2003 on which the braidplain morphology could be reliably identified. The inundated areas were automatically delineated using the color information of the Quickbird photograph and the elevation information of the DEM. The delineated polygons were then hand-edited to correct any misclassifications. We computed smoothed centrelines of the stream network polygon and we inserted segments perpendicular to the centrelines every 2 m. These segments were then clipped by the stream network polygon and used to assess the distribution of the width of the low-discharge stream. Furthermore, the water surface elevation of the stream network centrelines was extracted from the LiDAR-derived DEM and projected on the centreline of the braidplain. This procedure allows for a comparison of the elevation of the low-discharge streams and for examining their (vertical) positions within the braidplain. The longitudinal mean elevation and elevation range of the braidplain were estimated on the polygons formed by the area between two consecutive cross sections.

The lateral dynamics of braided river systems are known to be related to the transverse gradients of the braidplain that result from unequal sediment deposition (Ashmore, 1982; Bryant et al., 1995; Jones and Schumm, 1999; Ashworth et al., 2007). The transverse gradients were estimated by the slope of cross sections and by the slope of the local elevation minima of the same cross sections. Local elevation minima may act as local attractors that drain the water and sediment flows. Both types of transverse slopes were compared. To calculate the cross sections, a smoothed centreline of the braidplain corresponding to the longitudinal orientation of the braidplain was computed. Cross sections were traced at right angles to the centreline every 2 m. They were then clipped to the braidplain polygon, and the elevation information of the LiDAR-derived DEM was extracted for the cross sections.

The orthophotos were mainly used in association to the water-stage time-series to evaluate the morphological changes within the braidplain between 1998 and 2011. We focused on the high/active zone dynamics and on the reworking of the active zones.

3.4. Sedimentology

The sedimentological observations within the braidplain were limited to exposures (i.e., cut banks) above the water level. The sedimentary characteristics at the surface (e.g., coarse armor layer) can impact the transport initiation at low discharge but have likely little influence on the morphological shaping at high discharge (Bertoldi et al., 2010). Therefore, we do not focus on the sediment composition at the surface.

Exhaustive sedimentological observations over several years were made in different gravel pits of Pleistocene coarse deposits located in Switzerland (see also Siegenthaler and Huggenberger, 1993; Huggenberger et al., 1998; Beres et al., 1999; Regli et al., 2002; Huggenberger and Regli, 2006; Kock et al., 2009; Bayer et al., 2011). The observations were made on vertical sections at different stages of the wall excavations allowing the three-dimensional shape of the main sedimentological elements to be assessed with regard to the main former flow direction.

4. Results

4.1. Reach characterization

About 6% of the surface of the braidplain is vegetated, and 17% is inundated at the time of the Quickbird record (May 2005). We identified 11 large vegetation patch complexes. The topology of the low-discharge stream network corresponds to a partially connected network (see Fig. 1). Most of the low-discharge streams are connected in a reticulate/braided way (anabranch), but about 24 low-discharge streams are only connected to the network at the downstream end (i.e., pseudo anabranch or 'one-way connected stream with flowing water'; Arscott et al., 2002). The width of the low-discharge streams ranges from a few decimeters up to 100 m, the mean width being 24 m (Supplementary Fig. 3 online). We observed 100 ponds with elongated planform (5 length:width ratio on average) often found in local depressions (Supplementary Fig. 3 online). We counted about 60 ponds, each with an area $>100\ m^2$.

The mean longitudinal slope is almost constant (0.32%). After the removal of the longitudinal elevation trend, the low-relief topography shows height variations of up to 3.6 m over the whole reach. The average elevation difference over a radius of 10 m reaches 3 m, indicating locally large topographic gradients. The LiDAR-derived DEM (2005) consists of high zones surrounded by active zones. The high and active

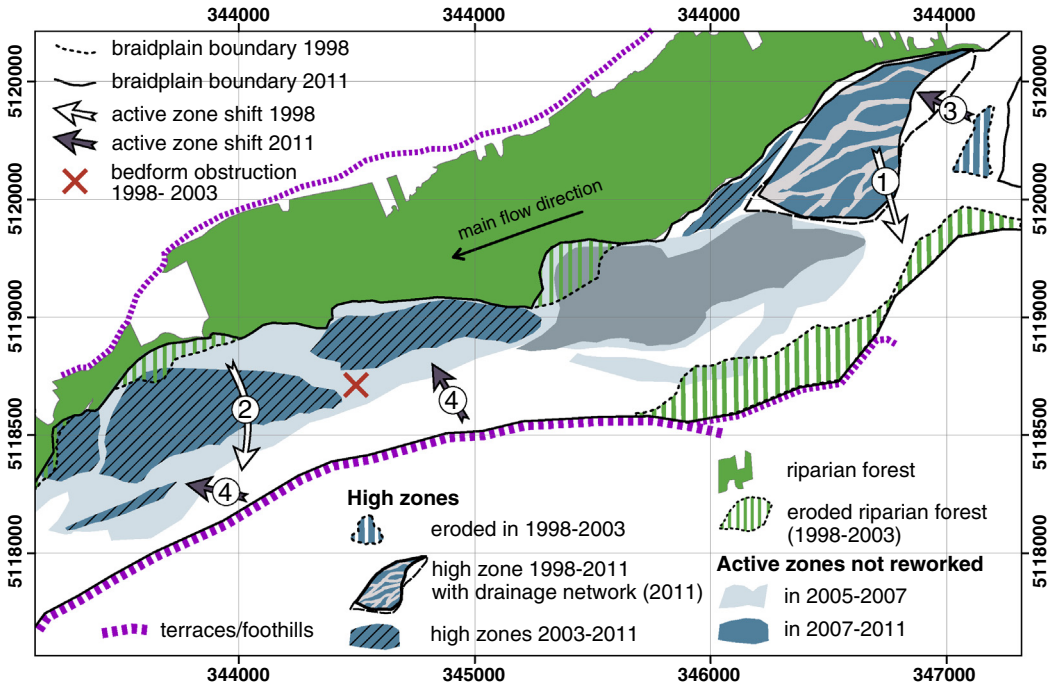

Fig. 3. Morphological development of the Tagliamento braidplain between 1998 and 2011. The numbers on the arrows identify the active zone shifts that are discussed in the text.

zones differ markedly not only in their relative elevation differences but also in their topographic signatures (see Fig. 1). The high zones lie about 1 to 2 m above the adjacent active zones and are on average 700 m long and 350 m wide. A drainage system incises 0.4 to 1.5 m below the top surfaces of the high zones and forms 1- to 35-m-wide gullies. Contrarily to the active zones, the high zones generally are vegetated. The active zones are characterized by the presence of gravel sheets and low-discharge streams.

4.2. High zone/active zone dynamics (1998–2011)

4.2.1. Braidplain evolution

The analysis of the aerial and satellite data shows that between 1998 and 2005 an active zone shift (active zone shifts ① and ② in Fig. 3) occurred toward the southwest boundary. This shift consisted in (i) the erosion of large area of riparian forest that can be presumably attributed to a flood event with a 32-year recurrence interval (the braidplain area increased by 9%; Fig. 4), (ii) the transformation of a large area of the active zone into a high zone (just downstream from the Cimano bridge), (iii) the formation of two high zones from relicts of former high zones (large vegetation patches) in the middle of the reach, and (iv) the obstruction of a large bedform (marked by an 'X' in Fig. 3) between these two newly formed high zones. Between 2005 and 2007, more than 50% of the braidplain was not reworked by the flows but still 15% of the high zone downstream from the Cimano bridge was eroded (active zone shift ③ in Fig. 3). Between 2007 and 2011, 35% of the braidplain was not reworked; and an active zone shift toward the northern boundary occurred in the middle of the reach (active zone shift ④ in Fig. 3). Fig. 4 shows, for the periods considered, the recurrence interval of the flood events as well as the areal proportions of the active/high zone combined with their reworked proportions.

4.2.2. High zone formation

The braidplain evolution from 1998 to 2011 shows how the high zone downstream from the Cimano bridge formed. Between 1998 and 2003, an area (0.5 × 1 km) within the active zone was more or less

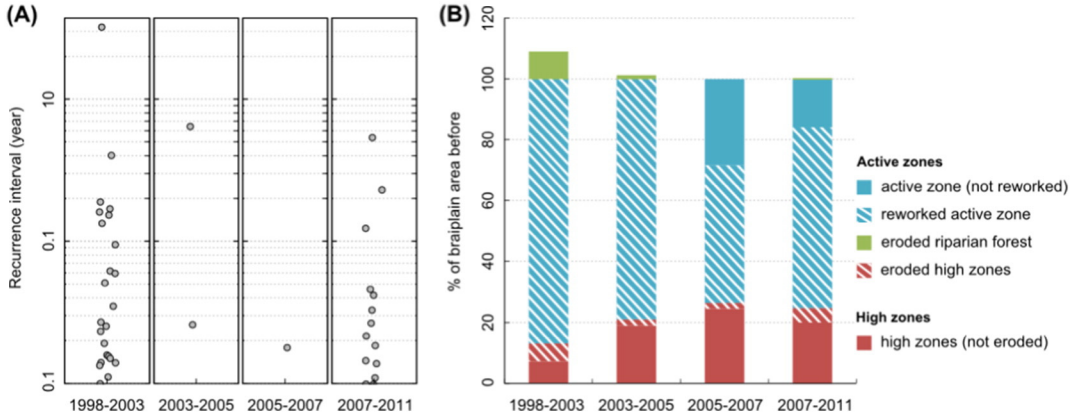

Fig. 4. For each time interval defined by the record time of the aerial/satellite photographs: (A) recurrence interval of the flood events larger than 0.1 year; (B) areal proportion of the high/active zone relative to the area of the braidplain at the beginning of the time interval.

abandoned by the river. That means that this area still experienced some erosion but was out of the discharges that would have completely reshaped it. Then vegetation developed, particularly at the edge of the highest locations. The hydraulic resistance of the vegetation to the flow further reshaped the abandoned area by inducing local scouring and sediment deposition (fine as well as coarse sediments) transforming the rather flat and smooth surfaces of the gravel sheets into a complex topography (see Gurnell et al. (2005) for more details on this process). Over time a dendritic drainage network that was not related to the abandoned morphology incised through the high zone and widened whereas the top surfaces of the high zone grew vertically by the deposition of trapped fine sediments. From 2003 onward, the high zone was further eroded at its edge by lateral scouring of the flow. The lateral scouring, often expressed in the form of cutbanks, can be seen as an instantaneous indicator for the current trend of lateral shift of the active zones. On the field between 2011 and 2014 we observed that the gravel substrate of the high zones lay higher than the surface of the surrounding active zones/gullies and that the height of the deposited fine sediments reached locally more than 1 m. The presence of mature vegetation is an indicator for high zones, although vegetation can colonize some parts of the active zones that are not reworked by the river over a given time period (as between 2007 and 2011).

4.2.3. Planimetry

The transverse slope computed on the whole cross sections shows a similar pattern as the transverse slope computed only on the local minima (Fig. 5). The upstream part of the reach is characterized by a dominant transverse slope toward the left side (southeast) of the braidplain with some locations where the transverse slope goes to zero. This slope direction corresponds to the location of the main active zones in the left side of the reach, indicating a relative stability; and it can result from the active zone shift observed between 1998 and 2005. Larger slope variations with changes of slope direction are observed in the downstream part of the reach. The observed relationship between the transverse slope and the braidplain width indicates the following trend: (i) the transverse slope is roughly inversely proportional to the width of the braidplain; and (ii) the transverse slope tends toward zero at the locations where the braidplain width is a local minimum (i.e., slight bottleneck locations).

The location of an area that is likely to experience a planimetric change in the near future under aggrading conditions is highlighted in Fig. 5. In this area, the location of the main active zone (southeast) does not correspond to the lowest positions as shown by the slope direction. Furthermore, we observed between 2007 and 2011 an active zone shift toward the northwest boundary in this area (active zone shift ④ in Fig. 3).

4.3. Morphology of the active zones

4.3.1. Gravel sheets

The principal bedform observed within the active zones is the gravel sheet. Only a few gravel sheets are very well preserved; the extent of about 30 gravel sheets is more or less recognizable over 100 relics of gravel sheets on the LiDAR-derived DEM as well as on the orthophoto from 2003. The length of these well-preserved gravel sheets ranges from 160 m up to 600 m and is proportional to their width (median width:length ratio ≈ 1.92, see Supplementary Fig. 4 online). The width of the gravel sheets is proportional to the width of the active zone. The avalanche face height ranges from centimeters up to 2 m (estimated average height from field observations and LiDAR-derived DEM analysis: 0.6 m). The gravel sheets delineated in 2003 and 2005 present no significant differences in size (Supplementary Fig. 4 online).

Fig. 6B and D shows a complex overlapping of remnants of gravel sheets with an orientation varying from north–south to east–west. Some of the gravel sheet remnants present low-discharge incisions with a depositional lobe at their front end. Furthermore, a low-discharge stream with a high curvature has strongly eroded this complex topography. The history of such highly superposed and reworked patterns is hardly reconstructable. In Fig. 6C and E a 1-m-thick, well-preserved gravel sheet (about 150 × 250 m) is dissected in its middle by a low-discharge incision (20 m wide and up to 1 m deep). This low-discharge incision deposited a lobe of sediment (60 × 25 m) at the edge of the gravel sheet into a large low-discharge stream. Another trace of dissection is also visible on the west side of the gravel sheet. The southeast edge of the gravel sheet is reworked by a sequence of edge collapses with depositional lobes. These lobes are called slip-face lobes (Rice et al., 2009) and are frequently found in sequences at the lateral edges of the gravel sheets where the transverse gradient is larger than

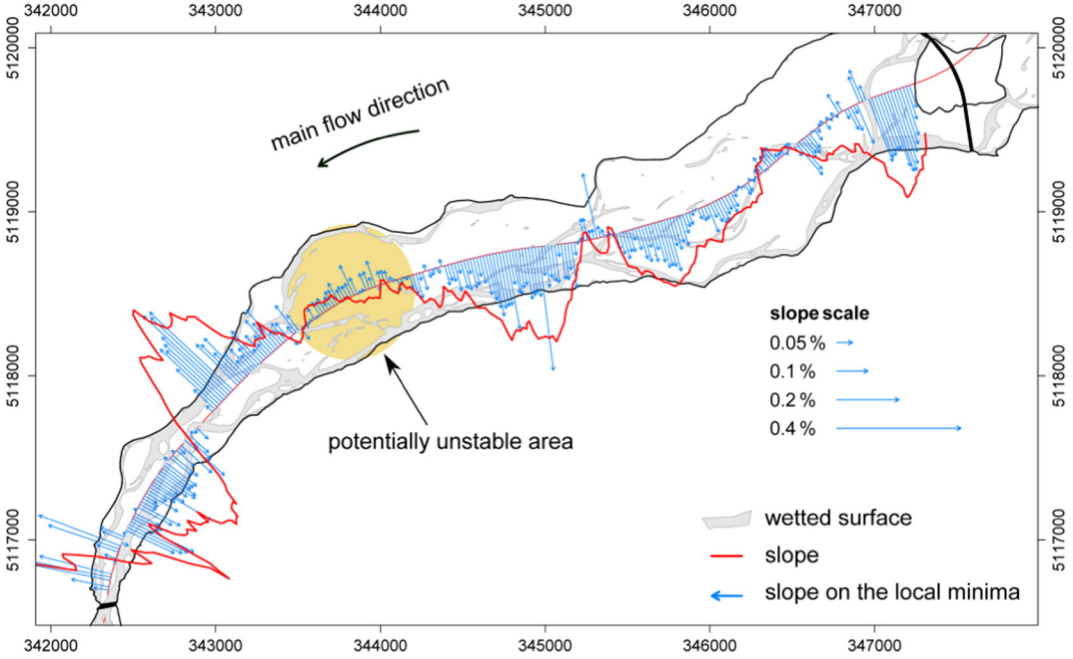

Fig. 5. Direction and magnitude of the lateral slope of the braidplain represented by arrows/lines. Two methods are compared: (i) the slope of the lateral cross sections and (ii) the slope of the local minima of the cross section.

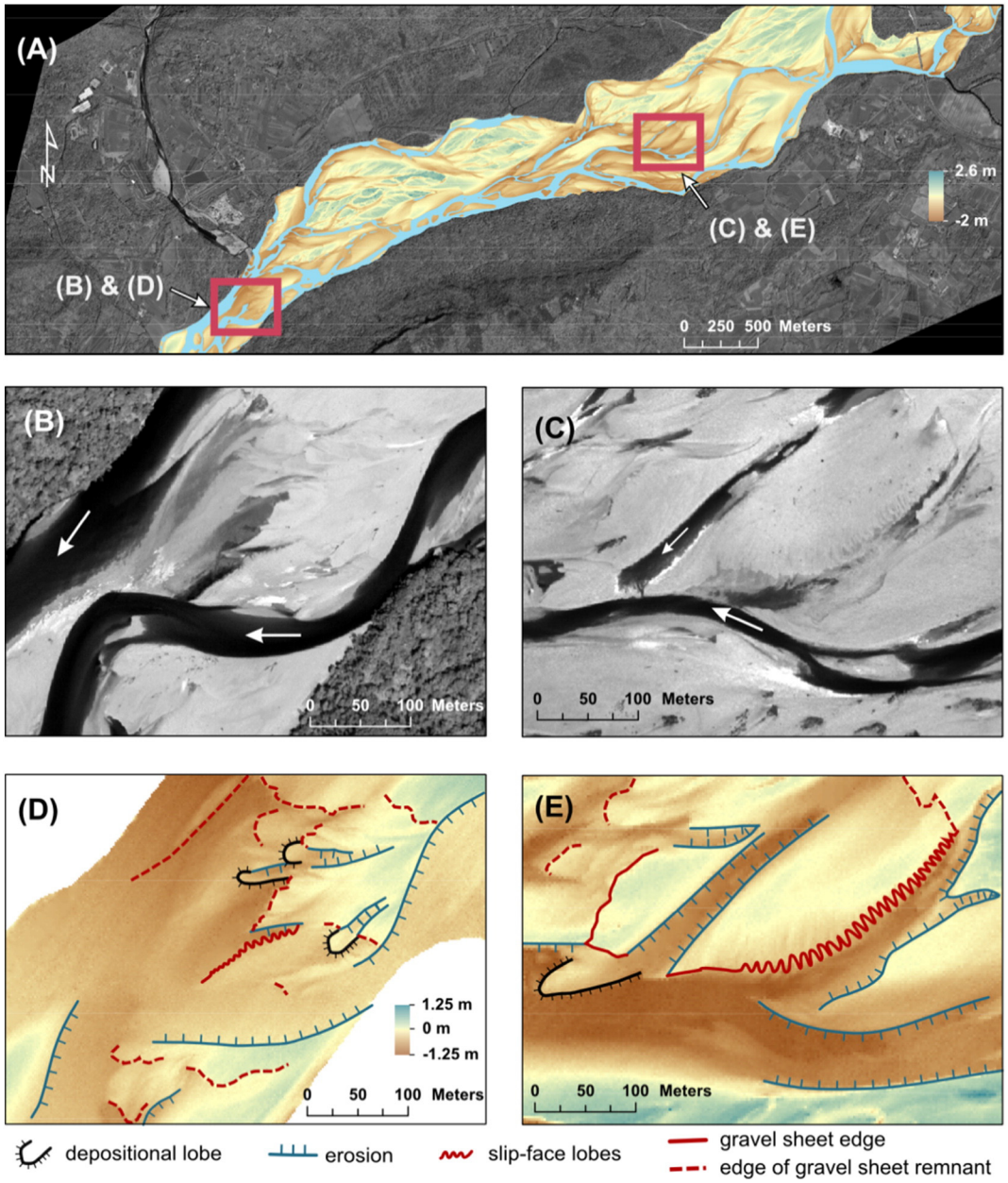

Fig. 6. Two examples of gravel sheet reworking and overlapping. (A) Position of the two locations in the braidplain (Quickbird photograph as background, relative DEM of the braidplain, delineated streams in blue). (B) and (C) Quickbird photograph. (D) and (E) LiDAR-derived DEM with superposed interpretations. Note that the Quickbird photograph and the LiDAR data were recorded in the same time and that they represent the same morphology.

the longitudinal gradient. Compare also the northeast to southwest orientation of the gravel sheet with the east to west orientation of the large low-discharge stream (Fig. 6C and E). These two different orientations mark the difference between the character of the river at high- and low-discharge conditions. Note also how much morphological information is gained from the LiDAR-derived DEM (compare Fig. 6 panels B and C with Fig. 6 panels D and E).

Furthermore, the gravel sheets can also be partially washed out by the flow, resulting in an armouring of their surface and/or smooth erosion that thins the gravel sheets and fuzzes their edges (e.g., the gravel sheet in Fig. 8C and D). Lateral accretion of the gravel sheets as well as the superimposition of thin gravel dunes on gravel sheets were not observed in the field or in the data.

4.3.2. Low-discharge streams and channels

Fig. 7A shows the projection of the water surface elevation of the low-discharge stream network and of the largest ponds on the centreline of the braidplain superimposed over the mean, minimum, and maximum elevation of the braidplain for each lateral polygon. The planform of the low-discharge stream network is represented in Fig. 7B. While the mean braidplain elevation shows a slightly upward-concave profile along the centreline, the minimum braidplain elevation presents a step-like pattern. The steps coincide with the location of bend erosion of the northern bank of the braidplain (compare Fig. 7A and B) highlighting the link between lateral erosion and scouring. Most of the branches of the projected low-discharge stream network also show a step-like pattern (step length: 200 ± 110 m, step height: 0.53 ± 0.23 m). The relative elevation between two low-discharge streams can strongly vary along the stream length (e.g., a higher-lying stream can end up as a lower-lying stream) indicating local variations of the potential energy between the low-discharge streams (i.e., topographic gradients). Differences in potential energy can drive morphological changes (e.g., avulsion). The elevation of the low-discharge streams is generally lower than the mean braidplain elevation, and in most cases

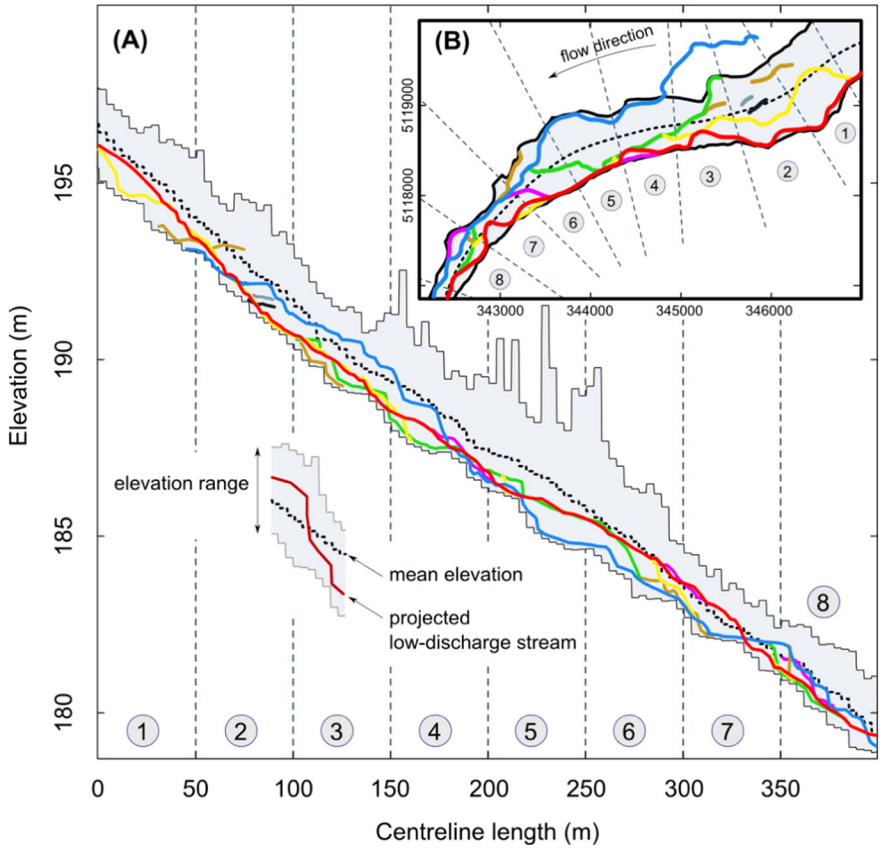

Fig. 7. (A) Elevation of the stream network projected on the centreline as function of the centreline length; (B) stream network planform with the braidplain boundaries. The centreline corresponds to the thick black dashed line.

a stream lies at the lowest location of the braidplain. The maximum elevation fluctuations reveal the presence of large higher-lying zones (large maximum elevation).

The morphology of the low-discharge channels is assessed by studying the topography of abandoned low-discharge streams on the LiDAR-derived DEM outside the reach. Based on the analysis of the topography (different cross-sectional geometry), we can distinguish two different types of low-discharge stream bed morphology: low-discharge incision and low-discharge channel.

The braidplain is locally overprinted by incisions often at the edges of gravel sheets but also through the gravel sheets (see Fig. 6). A closer look reveals a succession of steep and low gradient segments in the longitudinal direction: an incision into a morphological feature (strong topographic gradient) is followed by a plateau with sometimes small negative slopes where the low-discharge channel widens. The step-like longitudinal pattern of the low-discharge streams supports this observation (Fig. 7). Therefore, the length of the low-discharge incisions can be roughly inferred from the projected low-discharge stream network (e.g., 200 ± 110 m).

One to two main low-discharge channels with a light meander planform shape are identified on the LiDAR-derived DEM. They have a well-defined erosional surface with sharp boundary that is identifiable segment-wise in about 80% of the cases. These well-defined channel beds are only up to 0.5 m deep with regard to the lowest adjacent bank and between 10 and 50 m wide. They are wider than the low-discharge incisions. The elevation profile of the main channel shows an almost constant elevation profile (e.g., the stream in red in Fig. 5).

Traces of lateral accretion by low-discharge incision/channel migration are not visible in the field or in the data.

4.3.3. Scours

Interestingly, while scour fill structures can represent a large part of coarse-braided deposits (Siegenthaler and Huggenberger, 1993; Best and Ashworth, 1997), preserved scour holes were rarely observed in the studied reach.

The low-discharge stream confluences are rather low angle and not all of them form scours. Moreover, at some low-discharge stream confluences a slip-face lobe has been deposited from one tributary (e.g., Fig. 6C and E). On the orthophotos from 2003 to 2011, only one low-discharge stream confluence scour just downstream from the Cimano bridge is clearly visible through the clear water. This 50-m-long and 15-m-wide scour shows two avalanche faces at its upstream edges where the low-discharge streams enter into the confluence.

Between the edges of the gravel sheets and the confining structures, shallow ponds fed by groundwater exfiltration and large amounts of sand in association with sequences of slip-face lobes were often observed. Similar observations were also made between the edges of two gravel sheets. This can be attributed to the presence of filled scours that were formed at high discharge by flow turbulences induced by the braidplain topography. In the (dry) LiDAR-derived DEM, about 20 partially filled scours can be identified in the studied reach, which are up to 20 m wide, 180 m long, and 1 m deep (on average only 0.5 m deep) and have a trough rather than a spoon shape. They are located at the lowest parts of the floodplain.

Fig. 8 illustrates the lateral migration of a partially filled obstacle scour formed between the edges of a high zone and a gravel sheet. Between 1998 and 2011 the scour migrated over 80 m. On the DEM 2005, the water surface within the scour is almost at the same elevation as the water surface of the lowest low-discharge stream (Fig. 8G). We estimate the filled scour being up to 100 m long.

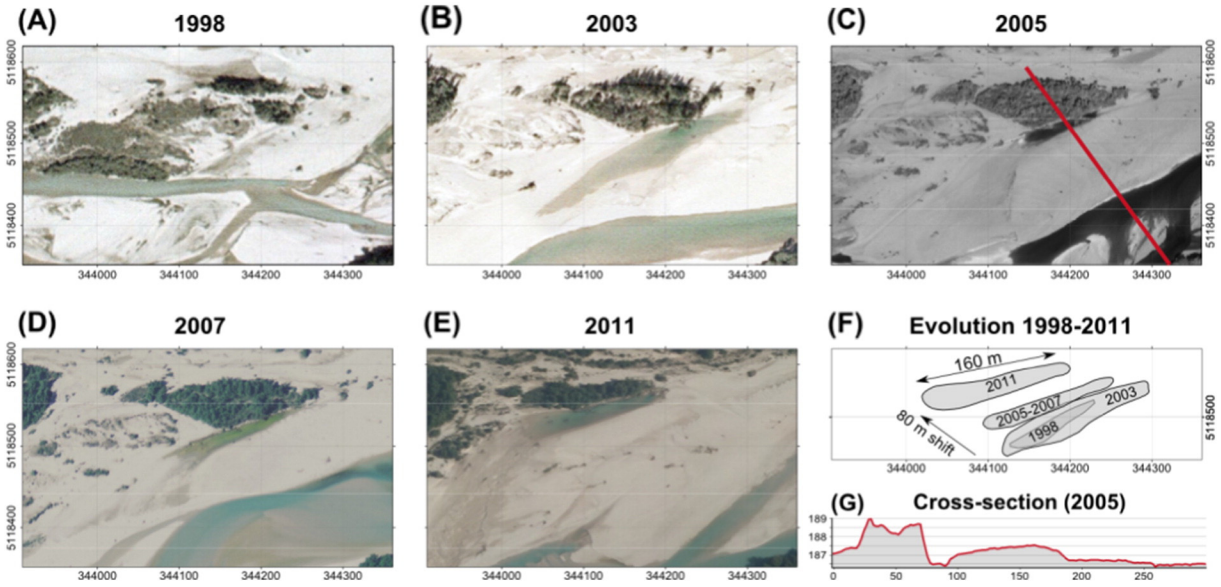

Fig. 8. (A)–(E) Migration of an obstacle scour between 1998 and 2011. The partially filled scours are identified by the local depression filled with water (except in 1998); (F) schematic migration of the local depression; (G) cross section of the LiDAR-derived DEM (2005) indicated by the red line on (C). Note that on (C) a well-preserved gravel sheet with an avalanche at its front edge lies between the obstacle scour and the low-discharge streams. The main flow direction is from upper right to lower left.

4.4. Geomorphological effectiveness of floods

4.4.1. High zones and riparian forest

In 13 years, 54% of the high zones from 1998 were eroded, mainly in 1998–2003 (45%). Large parts of riparian forest (9% of the 1998 braidplain area) were eroded in 1998–2003, most likely by the flood event with a 32-year recurrence interval (compare Fig. 4A and B). Even small events (e.g., events with recurrence intervals less than half a year) were able to rework the high zones, as between 2005 and 2007 where 7% of the high zones were eroded. Furthermore, other studies quantified a turnover rate of established islands (i.e., the vegetated part of the high zones) that was <25 years (e.g., Zanoni et al., 2008; Surian et al., 2015). Under the present conditions the life span of the high zones (and their vegetation) is limited up to 25 years by the lateral erosion of the river. The enhanced resistance of the vegetation to the flow seems only to postpone the (partial) erosion of the high zones until the next large flood event.

4.4.2. Active zones

Large flood events with a recurrence interval larger than 6.4 years completely reworked the active zones. Even small events (recurrence intervals <2 months) were able to partially rework the active zone (i.e., 45% of the active zone, see Fig. 4). Furthermore, the flood event from 31 October 2004 with a 6.4-year recurrence interval (314 cm water stage) was identified as having formed the gravel sheets in Fig. 6B–E and Fig. 8. The main gravel sheet observed in 2005 in Fig. 8 was presumably completely reworked by the flood event on 30 October 2008 with a 5.4-year recurrence interval (312 cm water stage). Between its formation and its complete destruction, we observe in 2007 the lateral erosion (up to 45 m) and *diffusion* (over max. 20 m) of the gravel sheet (Fig. 8D). The formation of slip-face lobes can be observed during the flow recession of the 20 January 2009 flood event (225 cm water stage; see the Supporting information in Bertoldi, 2012). On 22 January 2009 (159 cm water stage), a slight sequence of slip-face lobes is visible, and three days later (80 cm water stage) they were almost fully developed. Under the present conditions we expect that the active zones are completely reworked (e.g., formation of new gravel sheets and low-discharge incisions/channels) within <10 years (some of their parts being reworked more than once).

4.5. Sedimentary structure

4.5.1. Field observations (Tagliamento River)

Numerous exposures (i.e., cut banks) of partially/strongly reworked gravel sheets and of the high zones revealed a poorly sorted gravel texture with sometimes very low-angle horizontal bedding/coarse lags. The sediments on the avalanche faces of the gravel sheets are often rounded and grain supported.

4.5.2. Observations of gravel pit exposures (Switzerland)

In vertical outcrop exposures of ancient braided deposits, the depositional elements can be identified by (i) erosional bounding surfaces and (ii) sedimentary structures (i.e., one or two sedimentary textures that can alternate) and clast orientation (Siegenthaler and Huggenberger, 1993). Field observations of gravel pit exposures of Pleistocene coarse deposits in Switzerland (e.g., Fig. 9) showed that the main types of depositional elements are horizontal layers and 'cross-bedded sets […] with trough-shaped, erosional concave upward lower-bounding surfaces' (Huggenberger and Regli, 2006).

The horizontal layers correspond to poorly sorted gravels sometimes with horizontal beddings. The erosional bounding surface of the trough fills is generally spoon-shaped and oriented in the main flow direction. The trough fills mostly consist of open framework–bimodal gravel couplet cross-beds (see also Siegenthaler and Huggenberger, 1993; Huggenberger and Regli, 2006). No trough fills are observed at the top of the gravel pit exposures. A horizontal layer lies in most cases on top of the trough fills when the latter are not eroded by other trough fills. Surprisingly, small-scale incisions are almost absent from the deposits (see also Heinz et al., 2003).

The three-dimensional shapes of the trough fills are generally similar to the morphology of confluence scour holes. Some imbricated trough fills may be formed by multistage formative events, whereas the large widths of other trough fills suggest the migration of scours. The horizontal layers of poorly sorted gravel most likely originate from remnants of gravel sheets because the gravel sheet is the only geomorphological element that has a depositional character and is very extensive.

Fig. 9 shows a typical gravel pit exposure from the Hüntwangen site (northeast Switzerland) that is perpendicular to the former main flow

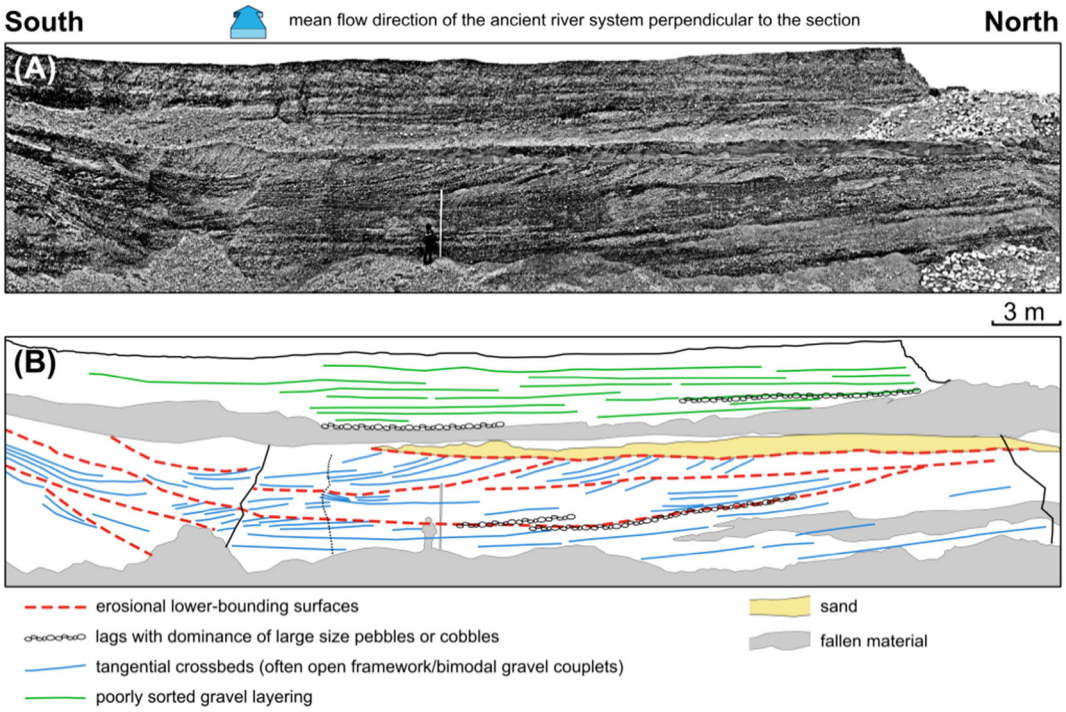

Fig. 9. (A) Gravel pit exposure (Huentwangen, northwest Switzerland) perpendicular to the former main flow direction. (B) Interpretation of (A). See the text for more details.

direction. The lower section of the exposure is characterized by the superposition of several trough fills identified by their erosional lower-bounding surfaces and their cross-bedding. The erosional lower-bounding surfaces indicate the erosional capacity of scouring. The top section of the exposure is dominated by poorly sorted gravel lacking in the fine sediment fraction. The layered aspect results from changing sand fraction and alternation of sand-free gravel. A few lags with dominant pebbles and cobbles indicate the reworking of the deposited gravel that left the coarse fraction. The former braided river dynamics can be partially inferred from the pattern of erosional lower-bounding surfaces as well as from their spatial density.

5. Discussion

5.1. High zones and active zones

A shift of the active zones toward the southwest associated with high zone formations (Fig. 3) was observed between 1998 and 2005. The period of generally low discharges (mainly between 2003 and 2007) and the fact that the gravel substrate of the high zone is higher than the surface of the surrounding active zones suggest a local entrenchment of the river. Because no sediment flux measurements are available, we do not know if the entrenchment resulted (i) from a large deposition of sediments before 2003 followed by a local incision of the active zone or (ii) from a local/unequal aggradation that increased the transverse gradient toward the southwest (Fig. 5) and occasioned the active zone shift. A regular monitoring of the topography would allow a better understanding of the active zone shifts and high zone formations in relation with the aggrading/degrading character of the reach and the transverse slope.

The topography of the active zones (e.g., the transverse slope, the confinement by the high zones) plays an important role by (i) controlling the stream power per unit width that impacts the sediment transport competence and capacity by the flows (Church, 2002) and (ii) conveying the flow toward obstacles (e.g., high zones) where the erosion process can operate by the abrasion of the obstacle with moving bedload particles (Sklar and Dietrich, 2004; Cook et al., 2014) and by scouring at the edge of the obstacle (Eilertsen and Hansen, 2007). In consequence, the active zone topography influences the geomorphological effectiveness of flood events. That can explain why small flood events (recurrence interval <2 months) were able to significantly erode the high zones between 2005 and 2007 (Fig. 4).

5.2. High-discharge/low-discharge morphologies

As highlighted in Section 4.3 (Fig. 6), the braided river morphology in the active zones — always observed during low-discharge — is the overprinting of a high-discharge morphology by a low-discharge morphology, both being the two extremes of a continuum (Church, 2002; Huggenberger and Regli, 2006).

The high-discharge morphology is built during flood events that partially reshape the braidplain: large gravel sheets form, are mobilized and transported, higher-lying zones are eroded, trees are uprooted, and the deepest scours are formed (Salter, 1993). Scours are produced by flow turbulences induced by topography especially near obstacles (e.g., along the side of the high zones; see Gurnell et al., 2005), between gravel sheets, and between the gravel sheets and the confining banks (Ashmore, 1982; Ashmore and Parker, 1983; Best and Roy, 1991). As the gravel sheets migrate during the flood event, the scours induced by the topography of the gravel sheets can also migrate longitudinally and transversely (see Ashmore and Gardner, 2008). The braidplain reshaping is largely determined by the discharge magnitude and duration and by the sediment pulses. The active zones are completely reshaped by high-energy events (recurrence interval larger than 6 years; Fig. 4) and still partially reshaped by low-energy events (recurrence interval <1 year). Periods of low discharges favor the vegetation development in the active zones that, in turn, favor the formation of a complex topography during flood events (e.g., Gurnell et al., 2005).

Field observations suggest that the low-discharge morphology is built during the hydrograph recession. The falling stage overprints a part of the high-discharge morphology with low-discharge incisions, lateral edge collapses of gravel sheets forming sequences of slip-face lobes, and sediment deposition (Fig. 6; see also Best and Roy, 1991; Bridge, 1993; Hicks et al., 2002, 2007; Bristow et al., 2009; Rice et al., 2009). A rapid decrease of the discharge increases the transverse hydraulic gradients compared to the longitudinal ones and thus favor

low-discharge incisions. In a laboratory experiment after the simulation of a flood event, Marti and Bezzola (2006) observed the formation of a large slightly meandering channel under low sediment supply conditions. This observation can explain the formation of the main low-discharge channels with their three-dimensional geometry that differs from the low-discharge incisions. The scours formed at high discharge are most probably covered by migrating gravel sheets (Ashmore and Gardner, 2008) and/or filled during the flow recession (Bridge, 1993). Storz-Peretz and Laronne (2013) assessed with buried chains scour-and-fill processes at confluences in a dryland braided river. They noticed that the scour holes formed during flood events were filled during the flow recession, and no evidence of their formation was detectable post-flood. This explains why scour holes are infrequently observed at low discharge and why the few observed (filled) scours are rather shallow. Interestingly, only a few low-discharge stream confluences form scours (see also Ashmore and Gardner, 2008).

In consequence, a correct decryption of the morphology must consider that (i) the braidplain observed at low discharge is always a combination of high- and low-discharge morphologies; (ii) the low-discharge morphology depends on the high-discharge morphology; and (iii) some high-discharge morphological elements (e.g., scours) can be indiscernible at low discharge.

5.3. Sedimentology

5.3.1. From morphological elements to depositional elements

The braidplain morphology observed at low discharge is a snapshot of a complex history that yields some clues to the erosional and depositional processes portrayed in vertical sections by erosional bounding surfaces. The formation of depositional elements is the result of either depositional (accretionary) processes or erosional and depositional (cut-and-fill) processes (Huggenberger and Regli, 2006) that create a morphology at a certain time.

The gravel sheets have a depositional character and a very low topography except at their edges. Because of the high river dynamics, we do not expect that complete gravel sheets will be entirely preserved in the sedimentary records (Smith, 1974). Rather, while the gravel sheets experience thinning and lateral erosion by the river, only remnants of gravel sheets are expected to be preserved in the subsurface. Parker et al. (2013) made a similar observation for sandy unit bar deposits and concluded that the identification of their remnants could be difficult. Smith (1974) observed on intact gravel sheets a general trend of upward grain-size fining, whereas he could not find evidence of a vertical grain-size trend on strongly reworked gravel sheets. In outcrops the poorly sorted gravel texture was identified with remnants of gravel sheets (Siegenthaler and Huggenberger, 1993; Beres et al., 1999; Heinz et al., 2003; Huggenberger and Regli, 2006; Benn and Evans, 2010).

The slip-face lobes and depositional lobes are erosional and depositional features with a small extent. The slip-face lobes lie at the lowest location of the braidplain where the river will flow during the next flood event. Therefore, the probability that the slip-face lobes will be preserved in the sedimentary records is nearly zero.

The formation, migration, and subsequent filling of the scours are erosional and depositional processes that create depositional elements, i.e., scour fills, characterized by sharp erosional lower-bounding surfaces and specific sedimentary textures resulting from the flow separation downstream of the avalanche faces of the scours (e.g., Ashmore and Gardner, 2008). The few identified scours at the surface are not representative of the abundance of scour fills in the near subsurface for the following reasons. (i) Most surely, some scours are completely covered by sediments (e.g., gravel sheets) and therefore are not identifiable at the surface (e.g., Bridge, 1993; Ashmore and Gardner, 2008; Storz-Peretz and Laronne, 2013). (ii) The migration of the scours creates erosional lower-bounding surfaces in the deposits that can be five times larger than the scour-hole surfaces observed at low discharge (Fig. 8; see also Heinz et al., 2003; Ashmore and Gardner, 2008). Scour fills were identified in outcrops by open framework–bimodal gravel couplet cross-beds and erosional lower-bounding surfaces (Siegenthaler and Huggenberger, 1993; Beres et al., 1999; Heinz et al., 2003; Huggenberger and Regli, 2006).

The low-discharge incisions and channels are shaped by erosional processes that can leave erosional lower-bounding surfaces in the near subsurface. The low-discharge incisions located on the gravel sheets are likely to be removed by the reworking of the gravel sheets. The low- discharge incisions/channels at the edges of the gravel sheets can be filled with sediments. Because the low-discharge incisions and channels are preferential flow paths, no flow separations and therefore no specific sediment sorting are expected to occur there. Rather, the low-discharge incision and channel fills likely consist of poorly sorted sediments from the gravel sheets and may be hardly distinguishable from the remnants of gravel sheets (Lunt et al., 2004). Ashworth et al. (2011) came to a similar conclusion for channel fill and *compound bar* deposits of the sandy braided South Saskatchewan River.

However, how the active zones are reworked by a large flood event with recurrence interval larger than 5 years is still unclear (i.e., how the gravel sheets form and migrate, and how aggradation occurs in relation with active zone shifts). We formulate two alternative working hypotheses: the pre-flood topography is either (1) covered by newly formed gravel sheets that migrate or (2) completely reworked up to a certain depth during the flood event followed by the formation and migration of gravel sheets. Compared to hypothesis (2), hypothesis (1) favors the preservation of the low-discharge morphology in the near subsurface.

Because the high zones develop from abandoned active zones, the sedimentary structure of the high zones corresponds to that of the active zone reworked by local erosion and gravel deposition, by the incision of drainage networks, and by the deposition of fine sediments. In consequence, the main depositional elements are gravel sheet deposits (poorly sorted gravel with possibly horizontal bedding), low-discharge incision/channel-fills (poorly sorted deposits similar to the remnant of gravel sheets), and scour fills (distinctive erosional lower-bounding surfaces in the deposits and cross-bed filling).

5.3.2. Preservation potential of the depositional elements

The preservation potential of a sedimentological unit in the sedimentary records is generally defined as the probability that the sedimentological unit will escape reworking (e.g., Meijer et al., 2008). The preservation potential of the depositional elements is a function of (i) their topographic positions (Siegenthaler and Huggenberger, 1993), (ii) their three-dimensional proportion (spatial density and shape), (iii) the aggrading/degrading character of the river, and (iv) the three-dimensional proportion of the other cut-and-fill depositional elements. During each formative event, the areal/volumetric proportion of the erosional elements at the lowest topographic positions (e.g., scours) combined with the rate of aggradation determine the preservation potential of the previously deposited elements (scour fills, gravel sheet deposits, low-discharge incision/channel fills, etc.). Note that the near-surface is not representative for the preservation potential of depositional elements as the near-surface is likely to still experience scouring by the river. The preservation potential can be confidently assessed at a depth below the deepest possible river erosion.

Section 4.4.1 shows that the high zones generally persist <25 years before they are eroded by the river. In aggradating settings, the high zones, particularly those that are stabilized by the vegetation, will be mainly scoured by the lateral migration of the active zones, resulting in pronounced erosional signatures in the subsurface. In case of high aggradation, the high zones could be buried and therefore partially preserved in the subsurface records. The preservation potential of the floodplain is similar to that of the vegetated high zones. Parts of the floodplain can be preserved if the rate of aggradation is large.

Table 1
Characteristics of the main depositional elements of a coarse, braided river.

Depositional element	Character	Areal proportion	Topographic level	Preservation potential	Hydraulic properties
Gravel sheet deposits	Depositional	Large	High	Low to large	Medium porosity & hydraulic conductivity
Scour fills	Erosional & depositional	Low to medium	Low	Largest	Large porosity & hydraulic conductivity
Incision/channel-fills	Erosional & depositional	Low to medium	Medium	Low to large	Medium porosity & hydraulic conductivity

Table 1 gives an overview of the characteristics of the main depositional elements of a coarse-braided river. The scour fills, by their low topographic level, have the largest preservation potential. If the low-discharge incisions/channels are preserved in the sedimentary records, they have a smaller preservation potential than the scour fills and a larger preservation potential than the gravel sheet deposits. However, small-scale depositional elements rarely appear on outcrop observations (see also Heinz et al., 2003). Either the low-discharge incision/channel fills can barely be distinguished from the adjacent poorly sorted deposits or the low-discharge incisions/channels are completely reworked when the active zones are reshaped by medium and large flood events. The preservation potential of the slip-face lobe deposits can be considered as null.

5.4. Hydrogeology

In a hydrogeological perspective, the scour fill deposits consisting of open framework–bimodal gravel couplet cross-beds contrast strongly with the other deposits in terms of hydraulic properties. Indeed, the open framework gravel texture is characterized by a very high hydraulic conductivity and porosity compared to the other sedimentary textures (e.g., Huggenberger et al., 1988; Jussel et al., 1994; Klingbeil et al., 1999; Heinz et al., 2003). Therefore, the three-dimensional spatial distribution of open-framework gravels in the subsurface is likely to act as a fast pathway for the subsurface flow. As a consequence, the high-discharge morphology, through its large preservation potential, hydraulically impacts much more the subsurface than the low-discharge morphology. The low-discharge morphology mainly produces discontinuities in the deposits that can be considered as noise that is immersed into the low to medium permeable deposits.

The length of the fast flow pathways is controlled by the size of the scour fills and their preservation. Long pathways are formed under high aggradation rates and high discharge dynamic conditions (i.e., frequent large flood events). Settings that favor a large proportion of highly permeable scour fill deposits and therefore a high density of erosion surfaces in the deposits are (i) a low aggradation rate and (ii) a large discharge dynamic (Table 2). However, under such settings, the connectivity of the open-framework gravel may be often interrupted by erosional lower-bounding surfaces, but still the largest quantity of subsurface water may flow through a small fraction of the deposits, the open-framework gravel. On the contrary, a high aggradation rate combined with a low-discharge dynamic increases the preservation potential of the gravel sheets as less scours are formed. Under low aggradation and low discharge dynamic, the low-discharge incisions might completely rework the high-discharge morphology (i.e., gravel sheets). An alternation of aggradation-degradation with an aggrading trend increases the subsurface heterogeneity compared to solely aggradation with the same trend.

Table 2
Relationship between surface dynamics and the abundance of depositional elements in the deposits: (++, +, +/−, −) stand for very large, large, medium, and low proportions.

		Aggradation rate	
		Low	High
Discharge dynamics	High	+ scour fills - remnant of gravel sheets +/- low-discharge incisions/channels	+/- scour fills + remnant of gravel sheets - low-discharge incisions/channels
	Low	+/- scour fills +/- remnant of gravel sheets + low-discharge incisions/channels	- scour fills ++ remnant of gravel sheets +/- low-discharge incisions/channels

6. Conclusion

This work aimed at characterizing the morphodynamics of a gravel-bed, braided reach (Tagliamento River) and at assessing its impact on the sedimentary deposits.

The surface morphology of the braidplain is not representative of the subsurface heterogeneity because (i) cut-and-fill processes such as scour formation, migration, and filling can leave no clues of their existence when the braidplain is observed at low discharge; (ii) the morphology at the highest position has the smallest preservation potential (e.g., the high zones are unlikely preserved in the subsurface even if they are stabilized by wooded vegetation, rather their erosion leaves erosional surfaces in the sedimentary records); (iii) the high-discharge morphology impacts more the hydraulic subsurface heterogeneity, but it is overprinted by the low-discharge morphology; and (iv) the near-subsurface that is more related to the morphology is likely to experience cut-and-fill processes in the future.

Therefore, the characterization of the subsurface structure through a pure morphological approach (e.g., topography stacking) underestimates the proportion of cut-and-fill depositional elements that are likely to control the fast pathways of the subsurface flow.

The qualitative preservation potential rules presented here could be implemented into a sedimentological stochastic model based on fuzzy logic. Different working hypotheses and settings regarding river dynamics could be considered, and the simulation outputs could be tested against vertical outcrop exposures. Further research should focus on the reworking of the active zones, more particularly on the processes behind the formation and migration of gravel sheets and scours over time, particularly at high discharge and during the hydrograph recession. These processes control the morphodynamic and the sedimentary processes.

Supplementary data to this article can be found online at http://dx.doi.org/10.1016/j.geomorph.2015.07.015.

Acknowledgments

This study was funded by the Swiss National Science Foundation within the ENSEMBLE project (grant no. CRSI22_132249/1). We thank A. Gurnel and W. Bertoldi who kindly provided us the LiDAR-derived DEM, M. Doering for the Quickbird photograph, and the Servizio Idraulica of the Autonomous Region of Friuli Venezia Giulia for the water stage timeseries. Special thanks go to L. Josset for constructive comments on a previous version of the manuscript. The critical comments from R.A. Marston and three anonymous reviewers helped to improve the quality of the manuscript.

References

Allen, J.R.L., 1978. Studies in fluviatile sedimentation: an exploratory quantitative model for the architecture of avulsion-controlled alluvial suites. Sediment. Geol. 21, 129–147. http://dx.doi.org/10.1016/0037-0738(78)90002-7.

American Society of Civil Engineers Task Force on Bed Forms in Alluvial Channels, 1966. Nomenclature for bedforms in alluvial channels. J. Hydraul. Div. ASCE 92, 51–64.

Anderson, M.P., 1989. Hydrogeologic facies models to delineate large-scale spatial trends in glacial and glaciofluvial sediments. Geol. Soc. Am. Bull. 101, 501–511. http://dx.doi.org/10.1029/95WR03399.

Anderson, M.P., Aiken, J.S., Webb, E.K., Mickelson, D.M., 1999. Sedimentology and hydrogeology of two braided stream deposits. Sediment. Geol. 129, 187–199. http://dx.doi.org/10.1016/S0037-0738(99)00015-9.

Arscott, D.B., Tockner, K., Van der Nat, D., Ward, J.V., 2002. Aquatic habitat dynamics along a braided alpine river ecosystem (Tagliamento River, Northeast Italy). Ecosystems 5, 802–814. http://dx.doi.org/10.1007/s10021-002-0192-7.

Ashmore, P.E., 1982. Laboratory modelling of gravel braided stream morphology. Earth Surf. Process. Landf. 7, 201–225. http://dx.doi.org/10.1002/esp.3290070301.

Ashmore, P., Gardner, J.T., 2008. Unconfined confluences in braided rivers. In: Rice, S.P., Roy, A.G., Rhoads, B.L. (Eds.), River Confluences, Tributaries and the Fluvial Network. John Wiley & Sons, Ltd, Chichester, UK, pp. 119–147 http://dx.doi.org/10.1002/9780470760383.ch7.

Ashmore, P., Parker, G., 1983. Confluence scour in coarse braided streams. Water Resour. Res. 19 (2), 392–402. http://dx.doi.org/10.1029/WR019i002p00392.

Ashworth, P.J., Best, J.L., Jones, M.A., 2007. The relationship between channel avulsion, flow occupancy and aggradation in braided rivers: insights from an experimental model. Sedimentology 54, 497–513. http://dx.doi.org/10.1111/j.1365-3091.2006.00845.x.

Ashworth, P.J., Sambrook Smith, G.H., Best, J.L., Bridge, J.S., Lane, S.N., Lunt, I.A., Reesink, A.J.H., Simpson, C.J., Thomas, R.E., 2011. Evolution and sedimentology of a channel fill in the sandy braided South Saskatchewan River and its comparison to the deposits of an adjacent compound bar. Sedimentology 58, 1860–1883. http://dx.doi.org/10.1111/j.1365-3091.2011.01242.x.

Bayer, P., Huggenberger, P., Renard, P., Comunian, A., 2011. Three-dimensional high resolution fluvio-glacial aquifer analog: part 1: field study. J. Hydrol. 405 (1–2), 1–9. http://dx.doi.org/10.1016/j.jhydrol.2011.03.038.

Bechtold, M., Battaglia, M., Tanner, D.C., Zuliani, D., 2009. Constraints on the active tectonics of the Friuli/NW Slovenia area from CGPS measurements and three-dimensional kinematic modelling. J. Geophys. Res. 114, B03408. http://dx.doi.org/10.1029/2008JB005638.

Benn, D.I., Evans, D.J.A., 2010. Glaciers and Glaciation. Second edition. Hodder Education, London 978-0-340-905791 (802 pp.).

Beres, M., Huggenberger, P., Green, A.G., Horstmeyer, H., 1999. Using two- and three-dimensional georadar methods to characterize glaciofluvial architecture. Sediment. Geol. 129 (1–2), 1–24. http://dx.doi.org/10.1016/S0037-0738(99)00053-6.

Bertoldi, W., 2012. Life of a bifurcation in a gravel-bed braided river. Earth Surf. Process. Landf. 37, 1327–1336. http://dx.doi.org/10.1002/esp.3279.

Bertoldi, W., Gurnell, A., Surian, N., Tockner, K., Zanoni, L., Ziliani, L., Zolezzi, G., 2009. Understanding reference processes: linkages between river flows, sediment dynamics and vegetated landforms along the Tagliamento River, Italy. River Res. Appl. 25 (5), 501–516. http://dx.doi.org/10.1002/rra.1233.

Bertoldi, W., Zanoni, L., Tubino, M., 2010. Assessment of morphological changes induced by flow and flood pulses in a gravel bed braided river: the Tagliamento River (Italy). Geomorphology 114 (3), 348–360. http://dx.doi.org/10.1016/j.geomorph.2009.07.017.

Bertoldi, W., Gurnell, A.M., Drake, N.A., 2011. The topographic signature of vegetation development along a braided river: results of a combined analysis of airborne lidar, color air photographs, and ground measurements. Water Resour. Res. 47, W06525. http://dx.doi.org/10.1029/2010WR010319.

Best, J.L., 1993. On the interactions between turbulent flow structure, sediment transport and bedform developments: some considerations from recent experimental research. In: Clifford, N.J., French, J.R., Hardisty, J. (Eds.), Turbulence: Perspectives on Flow and Sediment Transport. John Wiley & Sons, Ltd, Chichester, UK, pp. 61–93.

Best, J.L., Ashworth, P.J., 1997. Scour in large braided rivers and the recognition of sequence stratigraphic boundaries. Nature 387, 275–277. http://dx.doi.org/10.1038/387275a0.

Best, J.L., Roy, A.G., 1991. Mixing layer distortion at the confluence of channels at different depth. Nature 350, 411–413. http://dx.doi.org/10.1038/350411a0.

Best, J.L., Ashworth, P.J., Bristow, C., Roden, J., 2003. Three-dimensional sedimentary architecture of a large, mid-channel sand braid bar, Jamuna River, Bangladesh. J. Sediment. Res. 73, 516–530. http://dx.doi.org/10.1306/010603730516.

Bridge, J.S., 1993. The interaction between channel geometry, water flow, sediment transport and deposition in braided rivers. Geol. Soc. Lond., Spec. Publ. 75, 13–71. http://dx.doi.org/10.1144/GSL.SP.1993.075.01.02.

Bridge, J.S., Lunt, I.A., 2006. Depositional models of braided rivers. In: Sambrook Smith, G.H., Best, J.L., Bristow, C.S., Petts, G.E. (Eds.), Braided Rivers: Process, Deposits, Ecology and Management. Blackwell Publishing Ltd, Oxford, UK, pp. 11–49 http://dx.doi.org/10.1002/9781444304374.ch2.

Brierley, G.J., Fryirs, K.A., 2005. Geomorphology and River Management: Applications of the River Styles Framework. Blackwell Publishing, Oxford, UK (398 pp.).

Bristow, C.S., Jol, M.J., 2003. An introduction to ground penetrating radar in sediments. In: Bristow, C.S., Jol, M.J. (Eds.), Ground penetrating radar in sediments. Geol. Soc. Lond., Spec. Publ. 211, pp. 1–7.

Bristow, C.S., Best, J.L., Roy, A.G., 2009. Morphology and facies models of channel confluences. In: Marzo, M., Puigdefábregas, C. (Eds.), Alluvial Sedimentation. Blackwell Publishing Ltd, Oxford, UK, pp. 89–100 http://dx.doi.org/10.1002/9781444303995.ch8.

Bryant, M., Falk, P., Paola, C., 1995. Experimental study of avulsion frequency and rate of deposition. Geology 23 (4), 365–368. http://dx.doi.org/10.1130/0091-7613(1995)023<0365:ESOAFA>2.3.CO;2.

Burrato, P., Poli, M.E., Vannoli, P., Zanferrari, A., Basili, R., Galadini, F., 2008. Sources of Mw 5+ earthquakes in northeastern Italy and western Slovenia: an updated view based on geological and seismological evidence. Tectonophysics 453 (1–4), 157–176. http://dx.doi.org/10.1016/j.tecto.2007.07.009.

Church, M., 2002. Geomorphic thresholds in riverine landscapes. Freshw. Biol. 47 (4), 541–557. http://dx.doi.org/10.1046/j.1365-2427.2002.00919.x.

Colombera, L., Mountney, N.P., McCaffrey, W.D., 2013. A quantitative approach to fluvial facies models: methods and example results. Sedimentology 60, 1526–1558. http://dx.doi.org/10.1111/sed.12050.

Comunian, A., Renard, P., Straubhaar, J., Bayer, P., 2011. Three-dimensional high resolution fluvio-glacial aquifer analog — part 2: geostatistical modeling. J. Hydrol. 405, 10–23. http://dx.doi.org/10.1016/j.jhydrol.2011.03.037.

Cook, K.L., Turowski, J.M., Hovius, N., 2014. River gorge eradication by downstream sweep erosion. Nat. Geosci. 7, 682–686. http://dx.doi.org/10.1038/ngeo2224.

Cucchi, F., Finocchiaro, F., Muscio, G., 2010. Geositi del Friuli Venezia Giulia, Regione Autonoma Friuli Venezia Giulia. http://www.regione.fvg.it/rafvg/export/sites/default/RAFVG/ambiente-territorio/tutela-ambiente-gestione-risorse-naturali/FOGLIA201/FOGLIA18/allegati/Geositi_FVG_completo.zip (last accessed on 16th April 2015).

Eilertsen, R.S., Hansen, L., 2007. Morphology of river bed scours on a delta plain revealed by interferometric sonar. Geomorphology 94, 58–68.

Gurnell, A.M., Smith, B.P.G., Edwards, P.J., Kollmann, J., Ward, J.V., Tockner, K., Petts, G.E., Hannah, D.M., 2000. Wood storage within the active zone of a large European gravel-bed river. Geomorphology 34 (1–2), 55–72. http://dx.doi.org/10.1016/S0169-555X(99)00131-2.

Gurnell, A.M., Tockner, C., Edwards, P., Petts, G., 2005. Effects of deposited wood on biocomplexity of river corridors. Front. Ecol. Environ. 3 (7), 377–382. http://dx.doi.org/10.1890/1540-9295(2005)003[0377:EODWOB]2.0.CO;2.

Heinz, J., Kleineidam, S., Teutsch, G., Aigner, T., 2003. Heterogeneity patterns of Quaternary glaciofluvial gravel bodies (SW-Germany): application to hydrogeology. Sediment. Geol. 158 (1–2), 1–23. http://dx.doi.org/10.1016/S0037-0738(02)00239-7.

Heller, P., Paola, C., 1992. The large-scale dynamics of grain-size variation in alluvial basins, 2: application to syntectonic conglomerate. Basin Res. 4, 73–90. http://dx.doi.org/10.1111/j.1365-2117.1992.tb00146.x.

Hicks, D.M., Duncan, M.J., Walsh, J.M., Westaway, R.M., Lane, S.N., 2002. New views of the morphodynamics of large braided rivers from high-resolution topographic surveys and time-lapse video. The Structure, Function and Management of Fluvial Sedimentary Systems, No. 276. International Association of Hydrological Sciences, Wallingford, United Kingdom, pp. 373–380.

Hicks, D.M., Duncan, M.J., Lane, S.N., Tal, M., Westaway, R., 2007. 21 contemporary morphological change in braided gravel-bed rivers: new developments from field and laboratory studies, with particular reference to the influence of riparian vegetation. In: Helmut Habersack, H.P., Rinaldi, M., Rivers, Gravel-Bed (Eds.), VI: From Process Understanding to River Restoration. Elsevier, Amsterdam, pp. 557–584 http://dx.doi.org/10.1016/S0928-2025(07)11143-3.

Huggenberger, P., Aigner, T., 1999. Introduction to the special issue on aquifer-sedimentology: problems, perspectives and modern approaches. Sediment. Geol. 129 (3–4), 179–186. http://dx.doi.org/10.1016/S0037-0738(99)00101-3.

Huggenberger, P., Regli, C., 2006. A sedimentological model to characterize braided river deposits for hydrogeological applications. In: Sambrook Smith, G.H., Best, J.L., Bristow, C.S., Petts, G.E. (Eds.), Braided Rivers: Process, Deposits, Ecology and Management. Blackwell Publishing Ltd, Oxford, UK, pp. 51–74 http://dx.doi.org/10.1002/9781444304374.ch3.

Huggenberger, P., Siegenthaler, C., Stauffer, F., 1988. Grundwasserströmung in Schottern; Einfluss von Ablagerungsformen auf die Verteilung der Grundwasserfliessgeschwindigkeit. WasserWirtschaft 78 (5), 202–212.

Huggenberger, P., Hoehn, E., Beschta, R., Woessner, W., 1998. Abiotic aspects of channels and floodplains in riparian ecology. Freshw. Biol. 40 (3), 407–425. http://dx.doi.org/10.1046/j.1365-2427.1998.00371.x.

Jones, L.S., Schumm, S.A., 1999. Causes of avulsion: an overview. In: Smith, N.D., Rogers, J. (Eds.), Fluvial Sedimentology VI. Blackwell Publishing Ltd, Oxford, UK http://dx.doi.org/10.1002/9781444304213.ch13.

Jussel, P., Stauffer, F., Dracos, T., 1994. Transport modeling in heterogeneous aquifers: 1. statistical description and numerical generation of gravel deposits. Water Resour. Res. 30 (6), 1803–1817. http://dx.doi.org/10.1029/94WR00162.

Kelly, S., 2006. Scaling and hierarchy in braided rivers and their deposits: examples and implications for reservoir modelling. In: Sambrook Smith, G.H., Best, J.L., Bristow, C.S., Petts, G.E. (Eds.), Braided Rivers: Process, Deposits, Ecology and Management. Blackwell Publishing Ltd, Oxford, UK http://dx.doi.org/10.1002/9781444304374.ch4.

Klingbeil, R., Kleineidam, S., Asprion, U., Aigner, T., Teutsch, G., 1999. Relating lithofacies to hydrofacies: outcrop-based hydrogeological characterisation of quaternary gravel deposits. Sediment. Geol. 129 (3–4), 299–310. http://dx.doi.org/10.1016/S0037-0738(99)00067-6.

Kock, S., Huggenberger, P., Preusser, F., Rentzel, P., Wetzel, A., 2009. Formation and evolution of the Lower Terrace of the Rhine River in the area of Basel. Swiss J. Geosci. 102 (2), 307–321. http://dx.doi.org/10.1007/s00015-009-1325-1.

Lunt, I.A., Bridge, J.S., Tye, R.S., 2004. A quantitative, three-dimensional depositional model of gravelly braided rivers. Sedimentology 51 (3), 377–414. http://dx.doi.org/10.1111/j.1365-3091.2004.00627.x.

Mao, L., Surian, N., 2010. Observations on sediment mobility in a large gravel-bed river. Geomorphology 114 (3), 326–337. http://dx.doi.org/10.1016/j.geomorph.2009.07.015.

Marti, C., Bezzola, G.R., 2006. Bed load transport in braided gravel-bed rivers. In: Sambrook Smith, G.H., Best, J.L., Bristow, C.S., Petts, G.E. (Eds.), Braided Rivers: Process, Deposits, Ecology and Management. Blackwell Publishing Ltd, Oxford, UK, pp. 199–215 http://dx.doi.org/10.1002/9781444304374.ch9.

Meijer, X.D., Postma, G., Burrough, P.A., de Boer, P.L., 2008. Modelling the preservation of sedimentary deposits on passive continental margins during glacial–interglacial cycles. In: de Boer, P., Postma, G., van der Zwan, K., Burgess, P., Kukla, P. (Eds.), Analogue and Numerical Modelling of Sedimentary Systems: From Understanding to Prediction. Wiley-Blackwell, Oxford, UK http://dx.doi.org/10.1002/9781444303131.ch10.

Miall, A.D., 1985. Architectural-element analysis: a new method of facies analysis applied to fluvial deposits. Earth Sci. Rev. 22, 261–308.

Paola, C., Heller, P.L., Angevine, C.L., 1992. The large-scale dynamics of grain-size variation in alluvial basins, 1: theory. Basin Res. 4, 73–90.

Parker, N.O., Sambrook Smith, G.H., Ashworth, P.J., Best, J.L., Lane, S.N., Lunt, I.A., Simpson, C.J., Thomas, R., 2013. Quantification of the relation between surface morphodynamics and subsurface sedimentological product in sandy braided rivers. Sedimentology 60, 820–839. http://dx.doi.org/10.1111/j.1365-3091.2012.01364.x.

Petts, G.E., Gurnell, A.M., Gerrard, A.J., Hannah, D.M., Hansford, B., Morrissey, I., Edwards, P.J., Kollmann, J., Ward, J.V., Tockner, K., Smith, B.P.G., 2000. Longitudinal variations in exposed riverine sediments: a context for the ecology of the Fiume Tagliamento, Italy. Aquat. Conserv. Mar. Freshwat. Ecosyst. 10, 249–266. http://dx.doi.org/10.1002/1099-0755(200007/08)10:4<249::AID-AQC410>3.0.CO;2-R.

Pirot, G., Straubhaar, J., Renard, P., 2014. Simulation of braided river elevation model time series with multiple-point statistics. Geomorphology 214, 148–156. http://dx.doi.org/10.1016/j.geomorph.2014.01.022.

Ramanathan, R., Guin, A., Ritzi, R.W., Dominic, D.F., Freedman, V.L., Scheibe, T.D., Lunt, I.A., 2010. Simulating the heterogeneity in braided channel belt deposits: 1. A geometric-based methodology and code. Water Resour. Res. 46, W04515. http://dx.doi.org/10.1029/2009WR008111.

Regli, C., Huggenberger, P., Rauber, M., 2002. Interpretation of drill-core and georadar data of coarse gravel deposits. J. Hydrol. 255, 234–252. http://dx.doi.org/10.1016/S0022-1694(01)00531-5.

Rice, S.P., Church, M., Wooldridge, C.L., Hickin, E.J., 2009. Morphology and evolution of bars in a wandering gravel-bed river; lower Fraser river, British Columbia, Canada. Sedimentology 56 (3), 709–736. http://dx.doi.org/10.1111/j.1365-3091.2008.00994.x.

Salter, T., 1993. Fluvial scour and incision: models for their influence on the development of realistic reservoir geometries. Geol. Soc. Lond., Spec. Publ. 73, 33–51. http://dx.doi.org/10.1144/GSL.SP.1993.073.01.04.

Sambrook Smith, G.H., Best, J., Bristow, C., Petts, G., 2006. Braided rivers: where have we come in 10 years? Progress and future needs. In: Sambrook Smith, G.H., Best, J.L., Bristow, C.S., Petts, G.E. (Eds.), Braided Rivers: Process, Deposits, Ecology and Management. Blackwell Publishing Ltd, Oxford, UK, pp. 1–10 http://dx.doi.org/10.1002/9781444304374.ch1.

Siegenthaler, C., Huggenberger, P., 1993. Pleistocene Rhine gravel: deposits of a braided river system with dominant pool preservation. Geol. Soc. Lond., Spec. Publ. 75, 147–162. http://dx.doi.org/10.1144/GSL.SP.1993.075.01.09.

Sklar, L.S., Dietrich, W.E., 2004. A mechanistic model for river incision into bedrock by saltating bed load. Water Resour. Res. 40, W06301. http://dx.doi.org/10.1029/2003WR002496.

Smith, N.D., 1974. Sedimentology and bar formation in the Upper Kicking Horse River, a braided outwash stream. J. Geol. 82 (2), 205–223.

Storz-Peretz, Y., Laronne, J.B., 2013. Morphotextural characterization of dryland braided channels. Geol. Soc. Am. Bull. 125 (9–10), 1599–1617. http://dx.doi.org/10.1130/B30773.1.

Sun, A.Y., Ritzi, R.W., Sims, D.W., 2008. Characterization and modeling of spatial variability in a complex alluvial aquifer: implications on solute transport. Water Resour. Res. 44, W04402. http://dx.doi.org/10.1029/2007WR006119.

Surian, N., Barban, M., Ziliani, L., Monegato, G., Bertoldi, W., Comiti, F., 2015. Vegetation turnover in a braided river: frequency and effectiveness of floods of different magnitude. Earth Surf. Process. Landf. 40, 542–558. http://dx.doi.org/10.1002/esp.3660.

Todd, S.P., 1989. Stream-driven, high-density gravelly traction carpets: possible deposits in the Trabeg Conglomerate Formation, SW Ireland and some theoretical considerations of their origin. Sedimentology 36, 513–530. http://dx.doi.org/10.1111/j.1365-3091.1989.tb02083.x.

Van Der Nat, D., Tockner, K., Edwards, P.J., Ward, J.V., Gurnell, A.M., 2003. Habitat change in braided flood plains (Tagliamento, NE-Italy). Freshw. Biol. 48 (10), 1799–1812. http://dx.doi.org/10.1046/j.1365-2427.2003.01126.x.

Ward, J., Tockner, K., Edwards, P., Kollmann, J., Bretschko, G., Gurnell, A., Petts, G., Rossaro, B., 1999. A reference river system for the Alps: the 'Fiume Tagliamento'. Regul. Rivers Res. Manag. 15 (1–3), 63–75. http://dx.doi.org/10.1002/(SICI)1099-1646(199901/06)15:1/3<63::AID-RRR538>3.0.CO;2-F.

Webb, E.K., 1994. Simulating the three-dimensional distribution of sediment units in braided stream deposits. J. Sediment. Res. 64 (2b), 219–231.

Webb, E.K., Anderson, M.P., 1996. Simulation of preferential flow in three-dimensional, heterogeneous conductivity fields with realistic internal architecture. Water Resour. Res. 32 (3), 533–545. http://dx.doi.org/10.1029/95WR03399.

Welber, M., Bertoldi, W., Tubino, M., 2012. The response of braided planform configuration to flow variations, bed reworking and vegetation: the case of the Tagliamento River, Italy. Earth Surf. Process. Landf. 37, 572–582. http://dx.doi.org/10.1002/esp.3196.

Zanoni, L., Gurnell, A., Drake, N., Surian, N., 2008. Island dynamics in a braided river from analysis of historical maps and air photographs. River Res. Appl. 24 (8), 1141–1159. http://dx.doi.org/10.1002/rra.1086.